ANALYSIS AND EXPERIMENTAL CHARACTERIZATION OF IDLE TONES IN 2nd-ORDER BANDPASS ΣΔ MODULATORS – A 0.8μm CMOS SWITCHED-CURRENT CASE STUDY

José M. de la Rosa, Belén Pérez-Verdú, Fernando Medeiro, Rocío del Río and Angel Rodríguez-Vázquez

Instituto de Microelectrónica de Sevilla, IMSE (CNM-CSIC)
Edif. CNM-CICA, Avda. Reina Mercedes s/n, 41012 Sevilla, SPAIN
Phone: +34 95056666, FAX: +34 95056686, E-mail: jrosa@imse.cnm.es

ABSTRACT

This paper analyses the tonal behaviour of the quantization noise in 2nd-order bandpass ΣΔ modulators. The analysis previously performed for lowpass modulators is extended to the bandpass case. As a result, closed-form expressions for the frequency of the idle tones are derived for different locations of the signal center frequency. The analytical results are validated through measurements from a silicon prototype realized using fully differential switched-current circuits in a standard 0.8μm CMOS technology(*).

1. INTRODUCTION

Among other reasons, *Bandpass* ΣΔ Modulators (BP-ΣΔMs) [1] are of interest due to their suitability to realize the Analog-to-Digital (A/D) conversion of either Intermediate Frequency (IF) or Radio Frequency (RF) signals in modern digital radio receivers. Such A/D conversion permits the implementation of the IF stage in the digital domain, thus allowing digital control of the gain and the coefficients of the IF filter. This has numerous advantages as compared to the traditional (analog) radio receivers: reduction of interferences, programmability, etc...

Most reported BP-ΣΔMs obtain their architecture by applying a $z^{-1} \rightarrow -z^{-2}$ transformation to a *Lowpass* ΣΔ Modulator (LP-ΣΔM)[2][3]. Because of this transformation, a Lth-order LP-ΣΔM becomes a $2L$th-order BP-ΣΔM, keeping most of the properties of the former. One of these properties is the presence of *idle* tones in the output spectrum of the modulator. This phenomenon is caused by the correlation between the input signal and the quantization error [4]. The non-linear behaviour of the quantization error is more significant as the number of internal levels of the quantizer and/or the order of the modulator decrease, the worst case corresponding to a 1st-order LP-ΣΔM with a 1-bit quantizer.

The tonal behaviour of the quantization error in LP-ΣΔMs has been analysed elsewhere [5][6][7]. However, very little has been done currently for BP-ΣΔMs. In [8] a non-linear analysis of a 2nd-order BP-ΣΔM is reported assuming that the input is a sinusoidal signal with frequency equal to a quarter of the sampling frequency – the ideal signal-band center frequency. However, as we demonstrated in [9], in practical circuits this center frequency becomes shifted due to the influence of circuit errors, and such shifting needs to be considered for realistic tonal behavior analysis.

Asides with the analytical considerations, this paper shows experimental evidence of the tonal behavior of a 2nd-order BP-ΣΔM silicon prototype. The demonstration vehicle is a fully differential *switched-current* (SI) circuit, realized in a 0.8μm, standard CMOS technology. Measurements show that the results obtained for LP-ΣΔMs [5] can be extended to the bandpass case in order to explain the tonal behaviour of the quantization error in BP-ΣΔMs.

(*)This work has been supported by the Spanish CICYT Project TIC 97-0580

2. IDEAL ANALYSIS OF 2nd-ORDER BP-ΣΔMs

Fig.1(a) shows the block diagram of a 2nd-order BP-ΣΔM. It has been obtained by applying a $z^{-1} \rightarrow -z^{-2}$ transformation to a 1st-order LP-ΣΔM. As a consequence of this transformation, the original integrator becomes a resonator. Thus, the first step towards the design of a BP-ΣΔM is choosing a suitable architecture to realize the resonator transfer function. This can be realized using different topologies [2]. In this paper we will adopt a structure consisting of a feedback cascade of two *Lossless Discrete Integrators* (LDI), shown in Fig.1(b), where $A_F = 1$ and $A_{FB} = 2$. This structure has been chosen because it keeps the poles inside the unit circle upon changes due to errors of the feedback loop gain. However, the use of this resonator requires an additional delay block to be included in the digital loop, see Fig.1(a), in order to achieve the required delay in the modulator feedback loop.

2.1 Linear analysis

Assuming that the quantization error is modelled as an additive *white* noise source, the quantizer can be replaced by the linear model shown in Fig.1(c) [6][7]. In such a case, the modulator in Fig.1(a) can be viewed as a two-input, x and e, one output, y, system, which in the Z-domain can be represented by:

$$Y(z) = S_{TF}(z)X(z) + N_{TF}(z)E(z) \qquad (1)$$

where $S_{TF}(z)$ and $N_{TF}(z)$ are the signal transfer function and the noise transfer function, respectively,

$$S_{TF}(z) = z^{-1} \qquad N_{TF}(z) = 1 + z^{-2} \qquad (2)$$

By making $z = \exp(j2\pi f/f_s)$, where f_s is the sampling frequency, it can be shown that $N_{TF}(f)$ has one transmission zero at $f_s/4$, and that the filtering around this frequency is actually of the band-stop type. The input signal is allowed to pass while, at the same time, most of the quantization noise power is "shaped" so that is pushed out of the signal band. The *in-band* quantization noise power can be calculated by integrating the output Power Spectral

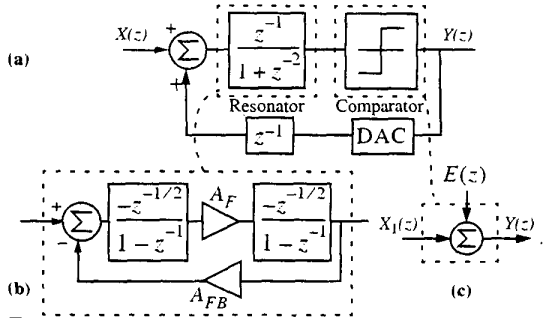

Figure 1. (a) Block diagram of the modulator in this paper. (b) LDI-loop resonator. (c) Linear model of the quantizer.

Density (PSD) within the signal bandwidth,

$$P_Q = \int_{f_s/4 - B_w/2}^{f_s/4 + B_w/2} 2S_Q |N_{TF}(f)|^2 df \equiv \frac{\Delta^2 \pi^2}{36M^3} \qquad (3)$$

where $S_Q = \Delta^2/(12f_s)$ is the PSD of the quantization noise, Δ is the quantization step, B_w is the signal bandwidth and $M \equiv f_s/(2B_w)$ is the *oversampling ratio*. From (3), and assuming that the modulator input is a sinewave of amplitude $A_x \leq \Delta/2$, the Signal-to-Noise Ratio (SNR) and the Dynamic Range (DR) are given by:

$$SNR \equiv \frac{A_x^2}{2P_Q} = \frac{18A_x^2M^3}{\pi^2\Delta^2} \qquad DR \equiv \frac{(\Delta/2)^2}{2P_Q} = \frac{9M^3}{2\pi^2} \qquad (4)$$

This ideal analysis shows that the modulator resolution increases with M at a rate of about 1.5-bit/octave. This ideal feature is achieved only if the resonator in Fig.1(b) is realized without errors and the quantization error is modeled by a white noise source.

2.2 Non-linear analysis

In the linear model shown in Fig.1(c), the quantization error, $e \equiv y - x_1$, is assumed to be not correlated with the quantizer input, x_1. Actually, this error is a non-linear function of x_1, as illustrated in Fig.2 for an N-bit quantizer†1.

If x_1 varies randomly from sample to sample in the interval $[x_{min}, x_{max}]$ (see Fig.2), e is largely uncorrelated with x_1 [4] and the linear model provides good results. This is achieved in LP-ΣΔMs for large modulator orders and $N > 1$ [7]. Therefore, the worst case for applying the linear model corresponds to a 1st-order modulator with a 1-bit quantizer. Candy [6] demonstrated that, for a dc input signal, the in-band quantization error power at the modulator output sharply changes with the input amplitude. This is illustrated in Fig.3(a) for $M = 64$ and $\Delta = 2$. This property of the quantization error, often known as *noise pattern*, is translated to a 2nd-order BP-ΣΔM when the input signal is a single tone placed at $f_s/4$. This is illustrated in Fig.3(b) by showing the simulated in-band quantization error power at the output of Fig.1(a) as a function of the input amplitude. This behaviour can not be explained by the linear model (dashed line in Fig.3(b)) and hence, a non-linear analysis is required.

Gray [5] solved the non-linear difference equations of a 1st-order LP-ΣΔM, showing that for dc inputs, the quantization error spectrum is discrete, with tones (often named *idle* tones) at

$$f_{tlp_n} = \langle n\left(\frac{1}{2} \pm \frac{A_x}{\Delta}\right)\rangle f_s \qquad \text{for } n = 1, 2, \ldots \qquad (5)$$

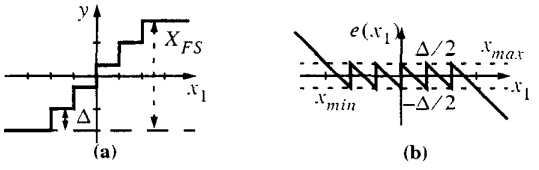

Figure 2. Ideal quantizer. (a) Input-output characteristics. (b) Quantization error.

†1. In the figure, X_{FS} stands for the full-scale range of the quantizer. Note that for $N = 1$, $X_{FS} = \Delta$.

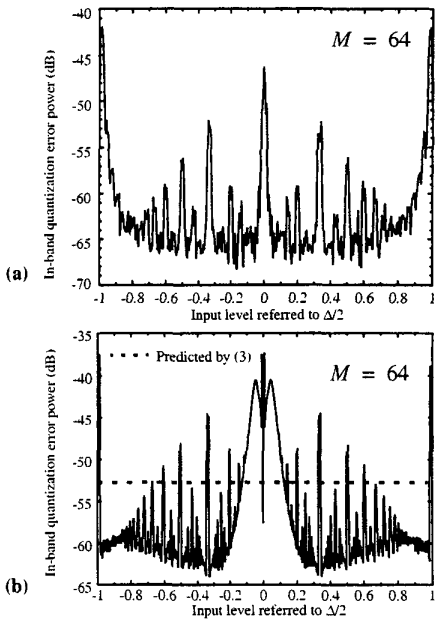

Figure 3. Noise pattern for a (a) 1st-order LP-ΣΔM and (b) 2nd-order BP-ΣΔM.

where A_x is the amplitude of x and $\langle a \rangle$ represents the fractional part of a. The amplitude of these tones is

$$A_{tlp_n} = \frac{1}{(2\pi n)^2} \qquad (6)$$

The above results can be extended to the bandpass case by applying the frequency translation dc $\rightarrow f_s/4$ to (5). This implies that the quantization error spectrum of a 2nd-order BP-ΣΔM with a sinusoidal signal placed at $f_s/4$ will have pairs of idle tones at

$$f_{tbp_n} = f_s \begin{cases} \langle n\left(\frac{1}{4} \pm \frac{A_x}{2\Delta}\right)\rangle \\ \langle n\left(\frac{1}{2} \pm \frac{A_x}{2\Delta}\right)\rangle \end{cases} \qquad \text{for } n = 1, 2, \ldots \qquad (7)$$

Note that there are tones placed around dc and $f_s/2$ – similar to the case of 1st-order LP-ΣΔMs. However, in 2nd-order BP-ΣΔMs there are also pairs of tones at both sides of $f_s/4$, the most significant being located at $f_s/4 \pm A_x/(2\Delta)$ as will be demonstrated experimentally in Section 4.

3. NON-IDEAL ANALYSIS – EFFECT OF SI ERRORS ON THE SIGNAL-BAND LOCATION

In the previous section the modulator was assumed to be ideal except for the inherent quantization error. In practice, circuit parasitics modify the zeroes of $N_{TF}(z)$, degrading the noise-shaping and making the in-band quantization noise to increase.

As we demonstrated in [9], errors in SI circuits cause the signal-band center frequency (often named *notch* frequency, f_{no}) to shift from its nominal position at $f_s/4$, causing an error denoted as δf_{no}, which is approximately given by:

$$\delta f_{no} \equiv f_{no} - \frac{f_s}{4} \cong -[(g_{oF} + g_{oFB})(2r_{on} + r_{in}) + 4\varepsilon_s]\frac{M}{\pi}\left(\frac{B_w}{2}\right) \quad (8)$$

where ε_s stands for the settling error [10], r_{in} is the input resistance of the memory cell, r_{on} is the steering switch-on resistance, and $g_{oF,FB}$ are the output conductances of the current mirrors used to realize the gains, $A_{F,FB}$, of the resonator in Fig.1(b).

Considering that the quantization noise power is minimum at f_{no}, the signal should be centered at f_{no} in order to obtain a maximum DR. On the other hand, placing a single tone at a frequency different from $f_s/4$ in a BP-ΣΔM is equivalent to applying a sinusoidal signal of low frequency in a LP-ΣΔM. As demonstrated in [5], the output spectrum of a 1st-order LP-ΣΔM with a sinusoidal input signal of frequency, f_i, is discrete, with tones at:

$$f_{tlp_n} = f_s \begin{cases} \langle n\frac{f_i}{f_s} \rangle \\ \langle n\frac{f_i}{f_s} - \frac{1}{2} \rangle \end{cases} \quad \text{for } n = 1, 2, 3, \ldots \quad (9)$$

This result can be extended to the bandpass case by applying the frequency translation dc $\rightarrow f_s/4$ to (9). This implies that the output spectrum of a 2nd-order BP-ΣΔM will have idle tones at:

$$f_{tbp_n} = f_s \begin{cases} \langle \left(\frac{1}{4} \pm n\frac{\delta f_{no}}{2}\right) \rangle \\ \langle \left(\frac{1}{2} \pm n\frac{\delta f_{no}}{2}\right) \rangle \end{cases} \quad \text{for } n = 1, 2 \ldots \quad (10)$$

Note that two families of tones appear at both sides of $f_s/4$, which can corrupt the signal information as will be demonstrated by experimental measurements in the next section.

4. EXPERIMENTAL RESULTS

The 2nd-order BP-ΣΔM of Fig.1(a) was realized using fully differential regulated-folded cascode memory cells. The 1-bit quantizer was made up of a regenerative latch and an RS flip-flop and the 1-bit DAC consisted of a current source controlled by the comparator output. These building blocks were designed to attaining the requirements of direct A/D conversion in AM digital radio receivers, whose commercial broadcast band is from 540kHz to 1.6MHz with stations occupying a 10kHz wide band. This imposes that the sampling frequency must be tunable over the range f_s = 2MHz to f_s = 6.4MHz.

The circuit was fabricated in a CMOS 0.8μm double-metal single-poly technology. Fig. 4 shows the microphotograph of the chip. It also includes some isolate building blocks for testing separately. The active area of the modulator is 0.35mm^2 and the power consumption is 42mW from a 5V power supply. To evaluate the performance of the modulator, it was attached to a two-layer test board, designed following the indications in [11] to reduce the switching noise. The output bit streams were captured with the HP82000 data acquisition system and Kaiser(β = 20)-windowed 32768-point FFTs were performed on each of those bit streams using MATLAB [12].

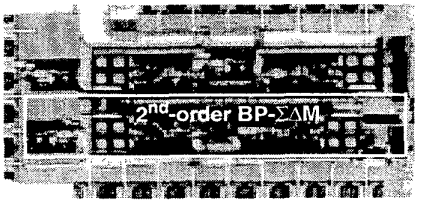

Figure 4. Microphotograph of the modulator.

4.1 Measurements for an input tone at $f_s/4$

Fig.5 shows two modulator output spectra when clocked at f_s = 2MHz. Note that, because of SI errors, f_{no} deviates from the ideal position at $f_s/4$. In this case, r_{in} = 2Ω, r_{on} = 472Ω, g_{oF} = 11μA/V, g_{oFB} = 21μA/V and ε_s = 250ppm, which according to (8), yields $f_{no} \cong 0.246 f_s$. As Fig.5 illustrates, there are four groups of idle tones whose frequencies are a function of the input signal amplitude. Note that, as A_x approaches to $\Delta/2$, two of these groups (labelled as L_1 and R_1 in Fig.5) move away from $f_s/4$ while the other two groups (L_2 and R_2) approach to $f_s/4$. The tones with the largest amplitude (≅−30dB) are those placed at:

$$f_{L1} = \frac{f_s}{4} - \frac{A_x}{2\Delta} f_s \qquad f_{R1} = \frac{f_s}{4} + \frac{A_x}{2\Delta} f_s$$
$$f_{L2} = \frac{A_x}{2\Delta} f_s \qquad f_{R2} = \frac{f_s}{2} - \frac{A_x}{2\Delta} f_s \quad (11)$$

which matches with that predicted by (7) for n = 1, as demonstrated in Fig.6 by displaying $f_{L1,2}$ and $f_{R1,2}$ vs. A_x/Δ, showing a good agreement between theory and measurements.

In AM radio applications, out-of-band idle tones are critical because, in the presence of non-linear errors, can mix with the input signal and fall into the signal band. For the special case of a single tone at $f_s/4$, the most significant intermodulation components (those corresponding to A_x approaching to Δ) will fall approxi-

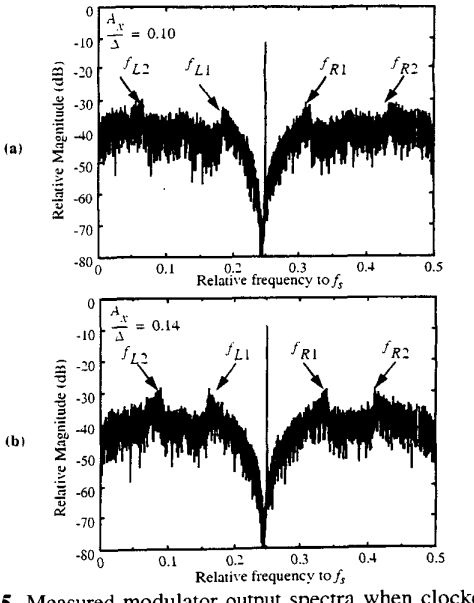

Figure 5. Measured modulator output spectra when clocked at f_s = 2MHz for an input tone of $f_s/4$ and different relative amplitudes: (a) A_x/Δ = 0.1, (b) A_x/Δ = 0.14.

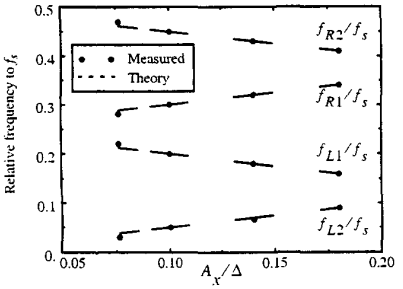

Figure 6. Idle-tone location vs. A_x/Δ for an input tone at $f_s/4$.

mately at $f_s/4$, thus not degrading the linearity of the modulator. However, in practical applications the input signal will contain spectral components at different frequencies, and according to (10), multiple tones will appear inside the signal band. This is verified by the following measurements.

4.2 Measurements for an input tone at f_{no}

Placing the input signal at f_{no} of a BP-ΣΔM maximizes the resolution of such a modulator. However, for the case of a 2nd-order BP-ΣΔM, a large number of idle tones will appear, thus destroying the operation of the modulator. Fig.7 illustrates this by plotting a measured modulator output spectrum when clocked at f_s = 2MHz corresponding to a single tone of −6dB input level[†2] and approximately located at the notch frequency.

According to (10), the frequency of idle tones only depends on the relative location of the input frequency with respect to $f_s/4$. However, as also shown in [5] for LP-ΣΔMs, the amplitude of such tones is strongly dependent on the input signal amplitude. Fig.8 illustrates this by plotting the central part of several measured output spectra corresponding to different input amplitudes. The position of the most significant tones (see (10)) are labelled. Observe that the amplitude of said tones is not a monotonic function of the input level, similarly to what happens to LP-ΣΔMs, in which the amplitude of idle tones is related to the input level through a linear combination of ordinary Bessel functions [5].

5. CONCLUSIONS

This paper demonstrated experimentally the strong correlation between the quantization noise and the input signal in 2nd-order

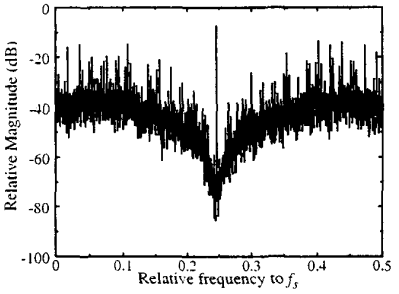

Figure 7. Measured modulator output spectrum for f_s = 2MHz and a −6dB input tone at 491kHz ($f_{no} = 0.246 f_s$).

†2. Input level is defined as the input signal amplitude referred to the DAC output level (= 0dB in the figure).

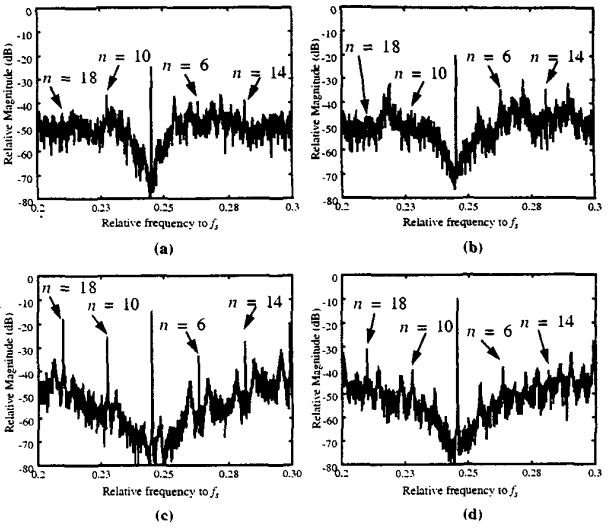

Figure 8. Measured modulator output spectra (central part) for an input tone at $f_{no} = 0.246 f_s$ ($\delta f_{no} = 0.0045 f_s$) and different relative amplitudes: (a) $A_x/\Delta = 0.03$. (b) $A_x/\Delta = 0.05$. (c) $A_x/\Delta = 0.1$, (d) $A_x/\Delta = 0.16$.

bandpass ΣΔ modulators. This phenomenon has been studied considering either that the noise shaping is ideal or it is degraded by circuit parasitics. As a result of this study, closed-form expressions for the frequency of idle tones have been derived regarding different cases of the signal center frequency. All results have been validated by measurements from a 0.8μm CMOS prototype.

REFERENCES

[1] R. Schreier and M. Snelgrove, "Bandpass Sigma-Delta Modulation", *Electronics Letters*, pp. 1560-1561, November 1989.

[2] F.W. Singor and W. M. Snelgrove, "Switched-Capacitor Bandpass Delta-Sigma A/D Modulation at 10.7 MHz", *IEEE J. Solid-State Circuits*, pp. 184-192, March 1995.

[3] A.K. Ong and B.A. Wooley, "A Two-Path Bandpass ΣΔ Modulator for Digital IF Extraction at 20MHz", *IEEE Journal of Solid-State Circuits*, pp. 1920-1933, December 1997.

[4] W. Bennett, "Spectra of Quantized Signals", Bell Syst. Tech. J., pp.446-472, July 1948.

[5] R.M. Gray, "Quantization noise spectra", *IEEE Transactions on Information Theory*, pp. 1220-1244, November 1990.

[6] J.C. Candy and G.C. Temes: "*Oversampling Delta-Sigma Data Converters*", IEEE Press, 1992.

[7] S.R. Norsworthy, R. Schreier, G.C. Temes: "*Delta-Sigma Converters. Theory, Design and Simulation*", New York, IEEE Press, 1997.

[8] T. Y. Chang and S. R. Ribyk, "Exact Analysis of Second-Order Bandpass Delta-Sigma Modulator with Sinusoidal Inputs", *Proc. 1999 IEEE Int. Symp. Circuits and System (ISCAS)*, Vol.2, pp. 372-375.

[9] J.M. de la Rosa, B. Pérez-Verdú, F. Medeiro, R. del Rio and A. Rodríguez-Vázquez, "Non-Ideal Quantization Noise Shaping in Switched-Current Bandpass Sigma-Delta Modulators", *Proc. of 1999 International Symposium on Circuits and Systems (ISCAS)*, Vol.2, pp. 476-479.

[10] C.Toumazou, J.B.Hughes, and N.C. Battersby, *Switched-Currents: An Analogue Technique for digital technology*, London, Peter Peregrinus Ltd.,1993.

[11] J.L. LaMay and H. T. Bogard, "How to Obtain Maximum Practical Performance from State-of-the-Art Delta-Sigma Analog-to-Digital Converters", *IEEE Trans. on Instrumentation and Measurement*, pp. 861-867, December 1992.

[12] *MATLAB: User's Guide*, The MathWorks Inc., 1991.